The International Journal of Advanced Manufacturing Technology (2018) 98:2987–3003
https://doi.org/10.1007/s00170-018-2470-3

ORIGINAL ARTICLE

Heat-assisted incremental sheet forming: a state-of-the-art review

Zhaobing Liu [1,2,3]

Received: 14 March 2018 / Accepted: 17 July 2018 / Published online: 26 July 2018

Abstract
Incremental sheet forming is an advanced manufacturing technique where a piece of sheet is shaped into a product by a series of small incremental localized deformations. It has revolutionized sheet shaping for small-batch production since its inception in the 1990s, providing an economical and effective alternative to sheet stamping and pressing, which are cumbersome and expensive. However, the materials with poor overall ductility at room temperatures are difficult to be formed by conventional incremental sheet forming. Therefore, several heat-assisted incremental sheet-forming methods have been developed by researchers trying to improve the formability of such materials and overcome the low geometrical accuracy as well. The aim of this paper is to provide a state-of-the-art review on the development of heat-assisted incremental sheet forming. It is hoped that the knowledge provided in this paper can facilitate readers working in this field to obtain a comprehensive view and take a step forward for future incremental forming of hard-to-deform materials at elevated temperatures.

Keywords Incremental sheet forming · Heat-assisted forming · Deformation · Hard-to-deform materials · Formability

1 Introduction

Incremental sheet forming (ISF), mainly referring to single-point incremental forming (SPIF) without a die and two-point incremental forming (TPIF) with a partial or full die, has gone through intensive research from academia and industries worldwide as a flexible sheet metal forming technology over the past decade. As a typical cold-forming process, materials can be formed by a series of localized plastic deformations at room temperatures. Among these tested materials, lightweight materials such as magnesium (Mg) and titanium (Ti) alloys have shown a growing interest in aerospace, automotive, and biomedical industrial applications. They are known as hard-to-deform materials with poor ductility at room temperatures. Therefore, the above mentioned "conventional" ISF (C-ISF) encounters difficulty in processing such kind of materials. To cope with this bottleneck, a range of "heat-assisted" ISF (HA-ISF) methods have been explored to overcome the limited formability and low geometrical accuracy of C-ISF.

Research work in the field of HA-ISF has been done in literature over the past decade. Nonetheless, it is difficult in having a comprehensive understanding due to disorganized and less linked scientific results obtained, although there exist a couple of review papers in ISF research [1–4]. With regard to this, the present paper aims at providing a concise summary of fundamentals and development of HA-ISF methods. In this way, industrial partners and researchers can benefit from this comprehensive review and overcome associated limitations and drawbacks in order to meet the future challenging in processing hard-to-deform materials by HA-ISF.

The structure of this paper is organized as follows: following this introduction section, the fundamentals on HA-ISF are described in Sect. 2. Furthermore, research methodology including analytical, numerical, and empirical modeling methods are presented in Sect. 3. Potential applications of HA-ISF are briefly envisaged in Sect. 4. Finally, conclusions and future directions are summarized and discussed, respectively in Sect. 5.

✉ Zhaobing Liu
zhaobingliu@whut.edu.cn; zhaobingliu@hotmail.com

[1] School of Mechanical and Electronic Engineering, Wuhan University of Technology, Wuhan 430070, China

[2] Institute of Advanced Materials and Manufacturing Technology, Wuhan University of Technology, Wuhan 430070, China

[3] Hubei Provincial Engineering Technology Research Center for Magnetic Suspension, Wuhan University of Technology, Wuhan 430070, China

2 Fundamentals of HA-ISF methods

Compared with C-ISF that is performed at room temperatures, HA-ISF can increase process formability, and reduce springback as well as forming forces when processing hard-to-deform materials such as Mg and Ti alloys. Based on different kinds of heat-generated sources, the heating methods in ISF are categorized and discussed in following subsections.

2.1 Laser heat

Laser, as an assisted heating source, has been incorporated into many manufacturing processes, which has also attracted attentions from ISF researchers [5–12]. In particular, Duflou et al. [5, 6] and Callebaut [7] introduced laser heating equipment to a robotic-based SPIF process, in which the laser beam moves with forming tool to locally heat the sheet metal. The experimental apparatus and corresponding cooling system are shown in Fig. 1a, b. Following the similar idea, Göttmann et al. [8] also developed an ISF system by integrating a coaxial rotating optics to the system. Furthermore, a PID-based control strategy was proposed by Göttmann et al. [9] to regulate the laser heat in order to ensure minimal temperatures needed in laser-assisted ISF process to achieve adequate formability of Ti grade 5. Mohammadi et al. [10–12] conducted series of researches towards formability and accuracy improvement of hard-to-work alloys formed by laser-assisted ISF. Transient heat transfer analysis was performed to simulate the laser movement during forming and further to retain proper process parameters for laser forming setup. The effect of laser transformation hardening on the accuracy was also investigated. Results revealed that the appropriate use of hard martensitic bands in steel sheets could increase the process accuracy with reduction of an unwanted deformation.

The above-developed laser-assisted ISF processes have many advantages such as well-controlled heating zone and temperature. The disadvantage of laser-assisted ISF is that the hardware cost is much higher as compared to other processes.

2.2 Halogen lamp heat

Kim et al. [13] developed a local heating apparatus for ISF in which several halogen lamps moving with forming tool were designed to heat AZ31 sheet. The experimental setup is shown in Fig. 2. Formability was evaluated at various temperature ranges. The results have shown that the fracture height increases as temperature goes up. However, as a large part of the heating zone is outside the tool sheet contact area, the heating is not thoroughly localized.

2.3 Hot air heat

Hot air blowers were utilized by Ji et al. [14, 15] to globally heat AZ31 magnesium alloy sheets in ISF process. Results revealed that a dramatic increase in formability of AZ31 sheets could be achieved above 150 °C.

2.4 Oil heat

Galdos et al. [16] have designed an experimental configuration for HA-ISF in which AZ31B magnesium alloy has been globally heated by using hot fluid. The temperature of the thermal oil can be controlled by a temperature control unit, which is able to reach up to about 300 °C. The sheet metal can be heated indirectly by convection in the hot fluid medium. Figure 3 shows the experimental set-up used for oil heat-assisted SPIF. Microstructural investigations of the HA-ISF parts revealed that full recrystallization could be achieved at 250 °C, in which the maximum angle of 60°can be formed. However, the maximum reachable temperature, by applying

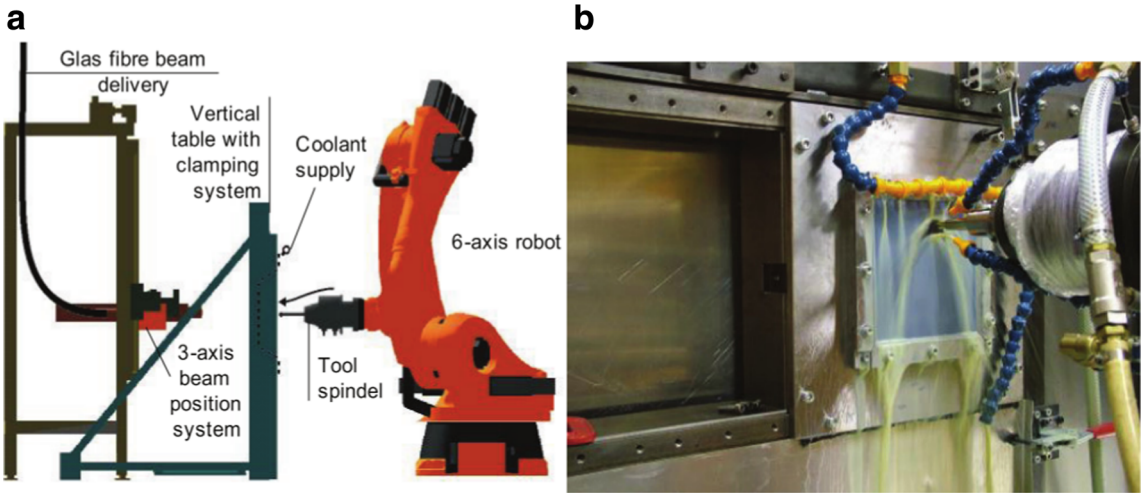

Fig. 1 **a** Robotic SPIF with laser heating. **b** Cooling/lubrication system [5]

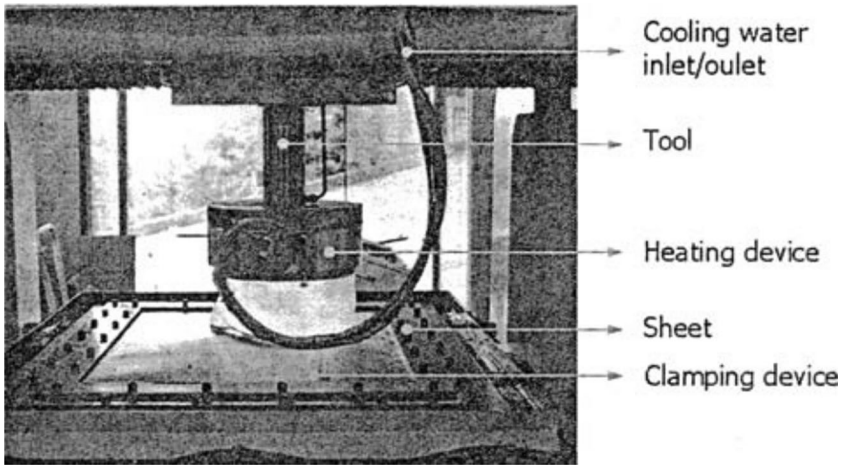

Fig. 2 Incremental forming at elevated temperature using halogen lamps [13]

hot oil, is limited, which can only be used for forming magnesium and aluminum alloys.

2.5 Friction heat

The high rotation speed of the forming tool can generate amount of friction heat, which can be utilized to improve the process formability [17–33]. The schematic view of fiction heat-assisted ISF is shown in Fig. 4. Durante et al. [17] systematically investigated the influence of tool rotation on SPIF in terms of forming forces, temperatures, and surface roughness. The tool rotation can decrease the forming force peaks. The highest level of temperature do not reach 60 °C as the maximum tool rotation speed is at 600 rpm. The formability has not been mentioned in their study. Park et al. [18] focused on forming limit improvement of magnesium alloy sheet by rotational ISF at room temperature. The tool with high rotation speeds generates local heat to accelerate plastic deformation. Additionally, the strain distribution of formed parts was obtained and compared with forming limit curve by considering the effect of tool radius, which is found to effectively predict the formability during rotational ISF of Mg alloy. Nguyen et al. [19, 20] further performed finite element analysis to predict the ductile fracture of Mg alloys for rotational ISF, which combines kinematic and isotropic hardening law. Otsu et al. [21, 22] employed the frictional heat generated between the rotating tool and the static sheet to improve the formability of Al alloys. Similar works can also be found in Buffa et al. [28], Baharudin et al. [31], and Uheida et al. [33], which deal with Al alloys (AA1050-O, AA1050-H24, AA6082-T6, and AA6061-T6) and Ti alloy, respectively. Xu et al. [23] investigated the influence of tool rotation and surface texturing on the formability in the frictional-stir ISF process. The formability behaviors under different tool rotation speeds were analyzed by grouping the speeds into four stages, revealing that friction plays a dominant role in low rotation speeds but thermal effect and potential dynamic recrystallization prevails at high rotation speeds. A further research by Xu et al. [24] was conducted to compare frictional-stir ISF with electric-assisted ISF. It is shown that frictional-stir ISF is more efficient but dependent on part geometry, while electric-assisted ISF has faster heating rate and less dependent on component geometry. Ambrogio et al. [25–27] investigated frictional-stir ISF of different lightweight alloys (Al and Ti alloys). A theoretical model was proposed to predict the temperature during forming using different process parameters, which provides

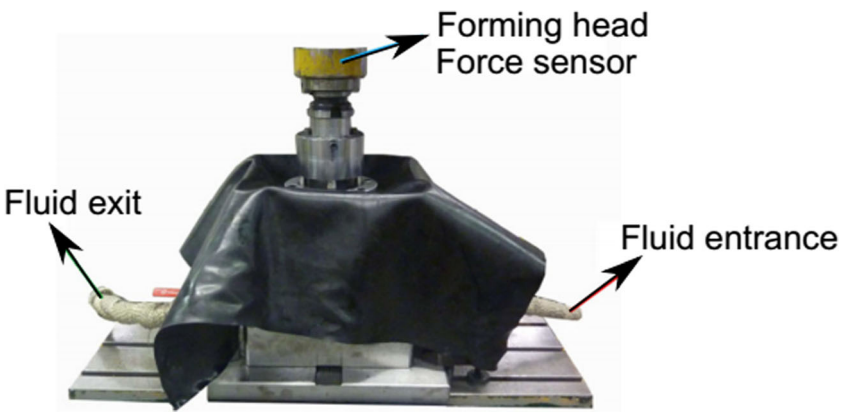

Fig. 3 Oil heat-assisted SPIF apparatus [16]

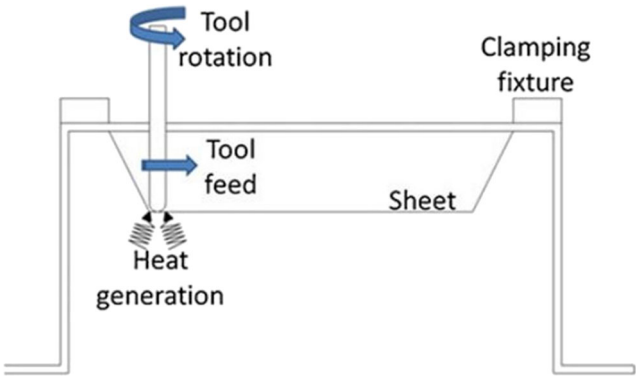

Fig. 4 Schematic view of friction heat-assisted ISF [32]

potentials for further analysis of material workability and microstructural evolution. Wang et al. [30] also discussed the effects of forming parameters on temperature in frictional-stir ISF based on experimental observations. Liu [32] performed a comprehensive analysis to evaluate the formability, surface quality, tensile strength, and micro-hardness of two typical parts formed by friction heat-assisted ISF. Experimental results revealed that the formability can enhance with the help of local frictional heating as well as the tensile strength and surface micro-hardness. Different from SPIF of metals, friction-stir ISF of polymers was discussed in Davarpanah et al. [29]. Effects of incremental depth and tool rotation on failure modes and microstructural properties were experimentally examined. It was found that higher tool rotation speed could lead to earlier occurrence of wrinkling of polymers. The friction heat-assisted ISF is easy to implement. However, uncontrollable forming temperature and severe tool wear are two major challenges.

2.6 Electric heat

Electrically assisted forming is a relatively new concept, in which the material properties of metals can be modified by applying electricity to the metal during deformation. In ISF, researchers introduced electricity directly or indirectly to heat the hard-to-deform alloys [34–55].

Ambrogio et al. [34] developed an electric heating system for forming the AZ31 sheets in the ISF process. In this system, a heater band was mounted at the external surface of the fixture. Experimental apparatus with electric band heater is shown in Fig. 5. Other than the local heating approach, this technology has to globally heat up the whole sheet during the forming process, which reduced the energy efficiency.

Fan et al. [36, 37] proposed an electric hot incremental sheet-forming process, as depicted in Fig. 6. Ambrogio et al. [35] further investigated this approach by quantifying the heat supplement respecting the forming parameters. A higher formability as compared to cold forming could be obtained. Microstructures and surface quality were also discussed. A different grain distribution and worse surface quality were witnessed due to electrical heating. Göttmann et al. [8] and Li et al. [49] tried to control the forming temperature by adjusting the input current. Adams and Jeswiet [42] investigated the electric ISF process and found out that the formability improvement of aluminum alloy 6061-T6 isattributed to a proper current density range. In the process, surface finish and geometric accuracy are the two major problems due to the extremely high temperature at a local area. Experimental investigations were widely adopted to understand the mechanism of the electric hot ISF of other alloys such as Ti alloy (Fan et al. [38], Khazaali et al. [45], Liu et al. [46], Najafabady et al. [47]) and Mg alloy (Le Van et al. [40], Bao et al. [43], Xu

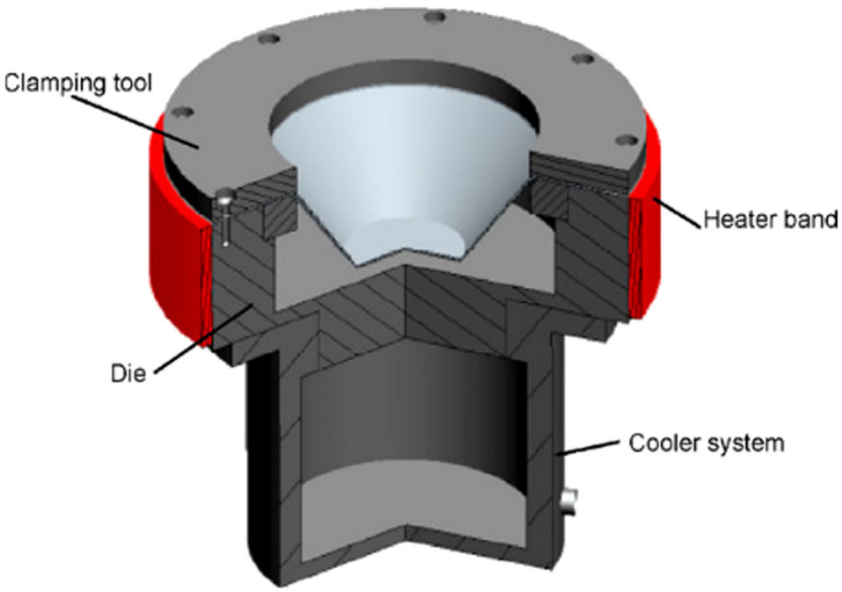

Fig. 5 Experimental apparatus with electric band heater [34]

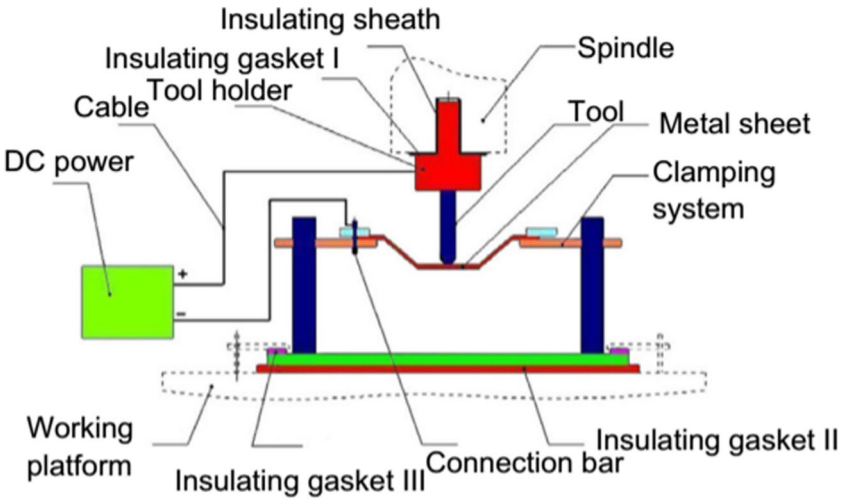

Fig. 6 Experimental principal of electric hot ISF with local heating [36]

et al. [48]). In these works, forming Ti alloy is much more difficult than other materials such as Mg and Al alloys, as higher temperature has to be used to deal with Ti alloy bringing challenges to better control the forming temperature. Given the limitations of local electric heating ISF discussed above, Li et al. [50] further proposed a new design for the integral electric heating ISF as shown in Fig. 7, aiming to improve the flexibility and defects (inhomogeneous temperature distribution, arc burns for the sheet and the tool, unsuited for multistage forming, and complex lubrication process) of local electric heating ISF. However, the integral electric heating ISF also has some problems, such as temperature monitoring, electrode heat management, and the effect of thermal expansion and contraction, needed to be solved.

In order to predict the electric heating ISF process, theoretical and FE models were developed to analyze the thermo-mechanical behavior in the forming process. Magnus [51] focused on the local electric heating of moving forming zone with up to two moving forming tools. A simplified model for temperature calculation has been established. In his subsequential work (Magnus [52]), the experimental setup was developed and forming of Ti6Al4V sheets was tested. Results showed reduced forming forces, spring-back, subsequent deformation of formed zones, and increased formability. Furthermore, the wear of tooltips (also discussed in Meier et al. [55]) and the metal sheet was presented, which could be kept at a relative low level when the forming temperature is properly controlled. Similar work can be found in Min et al. [53], in which a thermal model was also built including more than ten parameters to monitor the temperature and illustrate the effects of these parameters on the forming process. They claimed that the proposed model could be further integrated into the control algorithm to realize more accurate temperature control. Finite element models were also established to study the thermo-mechanical behavior of electric heating ISF in Fan et al. [39], Honapisheh et al. [44], and Pacheco et al. [54]. Through the numerical analysis, temperature distribution, thermal strain (stress), and equivalent strain could be revealed. More details are illustrated in Sect. 3.

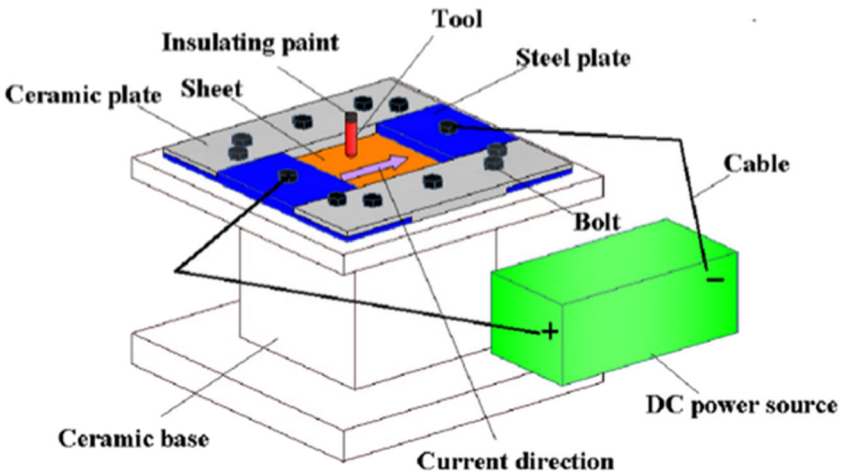

Fig. 7 Electric hot ISF with integral heating [50]

2.7 Induction heat

Induction heating appliance synchronizing with the tool movement during forming was proposed by Al-Obaidi et al. [56, 57]. The corresponding experimental setup is shown in Fig. 8. It enables the local heating of the AHSS sheet to elevated temperatures more than 850 °C, achieving improved formability, reduced remaining stresses, and forming forces. The similar research can also be found in Ambrogio et al. [58].

2.8 Combined (electric band + friction stir rotation) heat

Palumbo and Brandizzi [59] developed a process in which a static electricity heating was employed to pre-heat the sheets and then localized friction heating was superimposed to further increase the temperature. The experimental schematic view is shown in Fig. 9. A scaled automotive component in Ti6Al4V was successfully formed under a target temperature of 400 °C.

2.9 Summary of different HA-ISF methods

Details of different HA-IAF methods in terms of tested materials, lubricant used, and pros and cons since 2007 are summarized in Table 1.

3 Research methodology of HA-ISF process

Experimental investigations are widely adopted to study the HA-ISF process. However, it is difficult to understand the physical nature and deformation mechanism behind the ISF process with thermo-mechanical interaction. Therefore, analytical and numerical methods have been developed to model the HA-ISF process.

3.1 Analytical models

Ambrogio et al. [27] developed a mathematical model for friction heat-assisted SPIF aimed at predicting the temperature trends considering the influence of different process variables. The modeling approach involves the partitioning of the sheet metal being formed in points called nodes. The forming temperature variation ($\Delta T_{i,j}$) can be calculated for each node n_i and for each loop l_j using the equation below:

$$\Delta T_{i,j} = \frac{Q_{i,j} + \sum_{n_i \in N} q^j_{i,i'} + q^j_{i,p}}{c_p M_{i,j}} \quad (1)$$

where $Q_{i,j}$ is the heat generated on the node n_i during the loop l_j, $q^j_{i,p}$ and $q^j_{i,i'}$ are the heat exchanged by n_i with the punch and the other nodes, c_p is the specific heat of the material, and $M_{i,j}$ is the mass of the volume of the sheet in contact with the punch.

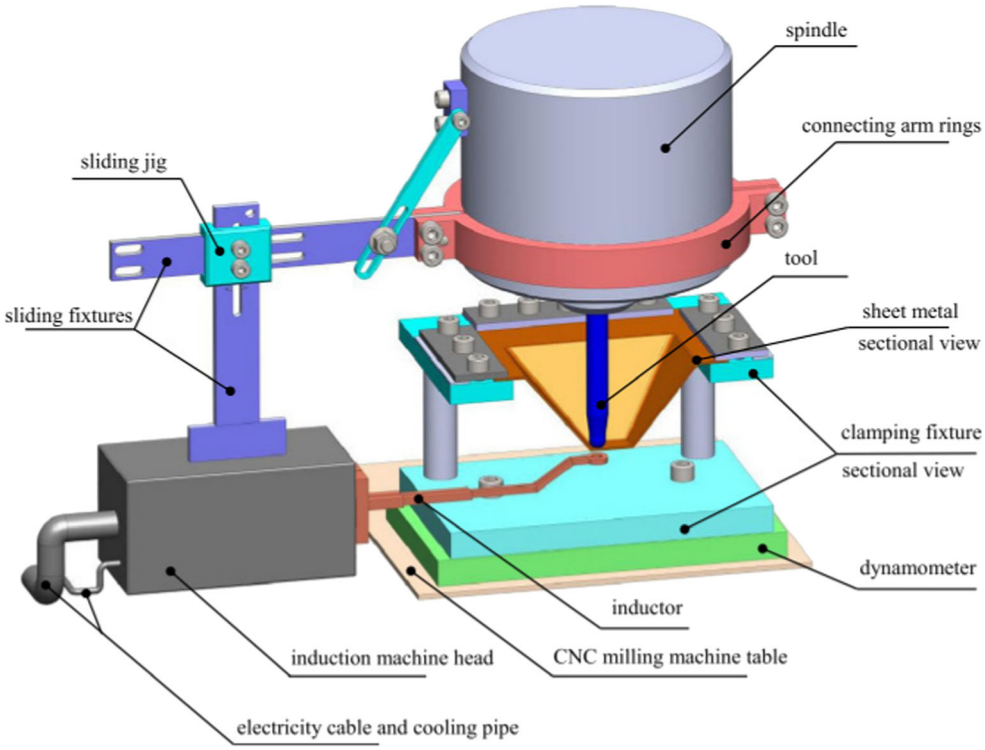

Fig. 8 Experimental setup for induction heat-assisted SPIF [56]

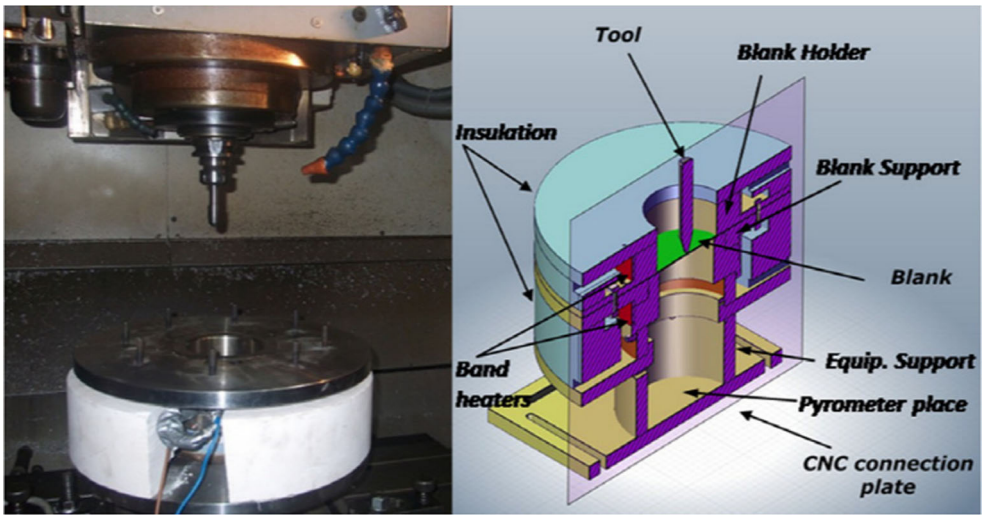

Fig. 9 Schematic view of SPIF setup with electric band heater [59]

Two materials were tested, of which AA5754 sheets were used to calibrate the established prediction model and Ti6Al4V sheets were used to validate the model. Results showed that the developed model was able to capture the temperature development during SPIF.

Fan et al. [36] first introduced the electric heating method to ISF, aiming to elevate the temperature of the contact field between the tool and hard-to-deform metal sheet. The thermal energy of local heating is calculated based on Joule's law and Ohm's law, which can be expressed as

$$Q = \int_0^t I^2(t) R_C(t) \mathrm{d}t \tag{2}$$

where $I(t)$ is the current, $R_C(t)$ is the contact resistance, and t is the electric time.

Magnus [51] derived a simplified analytical model for the development of the forming zone temperature in electric heat-assisted ISF process, which identifies the major process parameters on the temperature of the forming zone. The temperature of the forming zone ϑ_{fz} can be described as follows:

$$\vartheta_{fz} = \frac{I^2 R}{c_p \dot{m}} + \vartheta_1 \tag{3}$$

where ϑ_1 is the start temperature of the element to be heated; $c_p$is the material-specific heat capacity; $\dot{m}$ is the mass flow rate; $I$is electric current; $R$is the electric resistance.

In the further work of Magnus [52], results have shown that Joule heating of the dynamic forming zone in ISF can generate a high temperature gradient between the current forming zone and the rest of the sheet. A stable heating and forming process was achieved at up to 750 °C forming zone temperature when forming Ti6Al4V.

Min et al. [53] have also developed a thermal model for electric heat-assisted ISF process, which is a function of geometrical parameters of the sheet metal, process parameters, and the material property parameters. The temperature increase ΔT is given as follows:

$$\Delta T = \frac{I^2 R}{\overline{c} \cdot \overline{\rho} \cdot dV/d\tau} \tag{4}$$

where $\overline{c}$ and $\overline{\rho}$ are known material property parameters; $I$is electric current; R is the electric resistance; $dV/d\tau$ is the heated volume.

CP-K 60/78 and DP1000 steel were tested to validate the established thermal model. Results have shown that the tool radius and the wall angle have the most significant impacts on the temperature control through the electric current.

Li et al. [50] discussed the limitations of the local electric heating method in ISF and proposed a new global electric heating ISF. In this process, the heat generated by per unit volume of the sheet metal is analyzed according to the basic energy balance relation, which can be derived as

$$\int_V \rho \dot{U} dV + \int_V k \dot{\theta} dV = \int_V r dV - \int_{S_1} (q_1 + q_3) dS_1 - \int_{S_2} q_2 dS_2 \tag{5}$$

where ρ is the material density; $\dot{U}$ is the material time rate of the internal energy; k is the thermal conductivity of the metal sheet; $\dot{\theta}$ is the temperature gradient per unit volume; $q_1$and $q_3$are the heat flux of heat convection and radiation between the sheet and air; q_2 is the heat flux of heat convection between the sheet and the steel plate; $S_1$and S_2 are the contact surface area between the sheet and air and between the sheet and the steel plate, respectively.

3.2 Numerical models

The HA-ISF involves a relatively complex nonlinear thermomechanical coupling behavior which brings challenges

Table 1 Summary of different HA-ISF methods since 2007

HA-ISF methods	Refs.	Tested materials	Lubricant	Pros	Cons
Laser heat	Duflou et al. [5], [6]; Callebaut [7]; Göttmann et al. [8], [9]; Mohammadi et al. [10–12]	AA5182; 65Cr2; TiAl6V4; Ti Grade 2; AA2024-T3	Cooling lubricant; graphite; graphite "Berulit 935"	Well-controlled local heating zone; high heating temperature up to 600 °C	High hardware cost
Halogen lamp heat	Kim et al. [13]	AZ31	Liquefied synthetic oil with auto ignition point of 400	Low hardware cost; local heating	Heating zone is not thoroughly localized; low temperature less than 300 °C
Hot air heat	Ji et al. [14, 15]	AZ31	n.a.	Low hardware cost	Global heating cannot be easily controlled; low heating temperature less than 150 °C
Oil heat	Galdos et al. (2012) [16]	AZ31B	Oil 'Dynalene 600'	Low hardware cost; global heating but temperature can be easily controlled with a control system	Low reachable temperature less than 300 °C
Friction heat	Durante et al. [17]; Park et al. [18]; Nguyen et al. [19, 20]; Otsu et al. [21], [22]; Xu et al. [23], [24]; Ambrogio et al. [25], [26], [27]; Buffa et al. [28]; Davarpanah et al. [29]; Wang et al. [30]; Baharudin et al. [31]; Liu [32]; Uheida et al. [33]	AZ31; AZ61; AZ80; AA5052-H32; AA5052-H34; AA1050-O; AA1050-H24; AA5754; AA6061-T6; AA6082-T6; AA7075-O; Petroleum-based PVC; Bio-based PLA; Ti Grade 2; Ti6Al4V	MoS_2 + graphite; MoS_2; lithium-based grease	Local heating; reachable temperature above 600 °C	Uncontrollable forming temperature; severe tool wear; poor sheet surface quality
Electric heat	Ambrogio et al. [34], [35]; Fan et al. [36], [37], [38, 39]; Göttmann et al. [9]; Le and Nguyen [40]; Shi et al. [41]; Meier et al. [55]; Adams and Jeswiet [42]; Xu et al. [24], [48]; Bao et al. [43]; Honarpisheh et al. [44]; Khazaali and Fereshteh-Saniee [45]; Liu et al. [46]; Najafababy and Ghaei [47]; Li et al. [49], [50]; Magnus [51, 52]; Min et al. [53]; Pacheco and Silveira [54]	AZ31; AA1050; AA1060; AA2024-T3; AA5055; AA6061-T6; Ti6Al4V; CP-K 60/78 steel; TC4 Ti; low carbon steel DC01	MoS_2; graphite; MoS_2 + graphite; Ni-MoS_2; Oil "75 W-90"; Nickel alloy GH4169 and water cooling; "OKS280"; PTFE-based grease; mixture with MoS_2 and acetone solution	Local heating; reachable temperature up to 650 °C	Poor sheet surface quality; severe tool wear; complex lubrication needed
Induction heat	Al-Obaidi et al. [56], [57]; Ambrogio et al. [58]	DC04 low carbon steel; DP980 steel; 22MnB5 steel; HCT980C steel; DP1000 steel; Ti6Al4V	Cryogenic cooling with liquid nitrogen	Local heating; reachable temperature more than 850 °C; lower hardware cost compared to laser heating; better surface quality compared to electric heating	No obvious drawbacks
Combined heat (Friction + electric bands)	Palumbo and Brandizzi [59]	Ti6Al4V	"OKS280"	Low cost hardware (global heating by electric bands + local heating by friction)	Inhomogeneous temperature distribution (peripheral region is much higher than the central part); wear of tool and sheet surface

Table 1 (continued)

HA-ISF methods	Refs.	Tested materials	Lubricant	Pros	Cons
n/a	Zhang et al. [60], [61]	AZ31	MoS_2; graphite; $K_2Ti_4O_9$ + graphite; MoS_2, or graphite with pulsed anodic oxidation	Easy to implement	Global heating cannot be easily controlled; low temperature less than 250 °C

to the accurate analytical modeling of such forming process. The current established analytical models as illustrated in Sect. 3.1 are mostly focused on the temperature prediction in the electric heat-assisted ISF. For the HA-ISF processes, the material temperatures, dimensions, and properties are changing both in time and space depending on many process parameters, and the numerical approach is, therefore, more beneficial for modeling these situations. As the improvement in computational efficiency in recent years, numerical models established by commercial software such as ABAQUS and ANSYS for the thermomechanical studies are becoming more prevalent.

In the work by Mohammadi et al. [9], a transient heat transfer model was developed and incorporated into the FE model in ABAQUS to simulate the laser-assisted ISF. In their model, the laser beam was treated as a surface heat flux applied to a specific number of elements considering the size of the laser beam. It can further change its position in small-time increments according to the setting of the laser beam moving speed. The sheet was modeled using DC3D8 elements. Additionally, only the heat losses resulted from convection and radiation are taken into consideration in the FE model. The FE setup and FE results of temperature distributions are illustrated in Figs. 10 and 11, respectively. The influence of laser heat on the forming of a truncated cone was comprehensively analyzed.

Nguyen et al. [19, 20] investigated thermomechanical finite element modeling of the friction heat-assisted ISF. In their work, the Oyane's fracture criterion based on a combined kinematic/isotropic hardening law and Johnson-Cook model was used to predict the forming fracture at elevated temperatures generated by friction heat. The finite element model for friction heat-assisted ISF is shown in Fig. 12. In the model, only one-quarter of the sheet metal was modeled using solid elements C3D8R. The tool and die were modeled using rigid surface elements R3D4. It is noted that the tool was allowed to move along the tool path

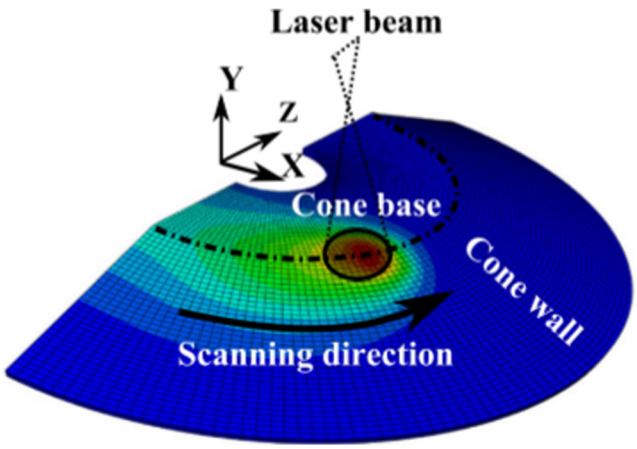

Fig. 10 Schematic illustration of laser-assisted incremental forming [9]

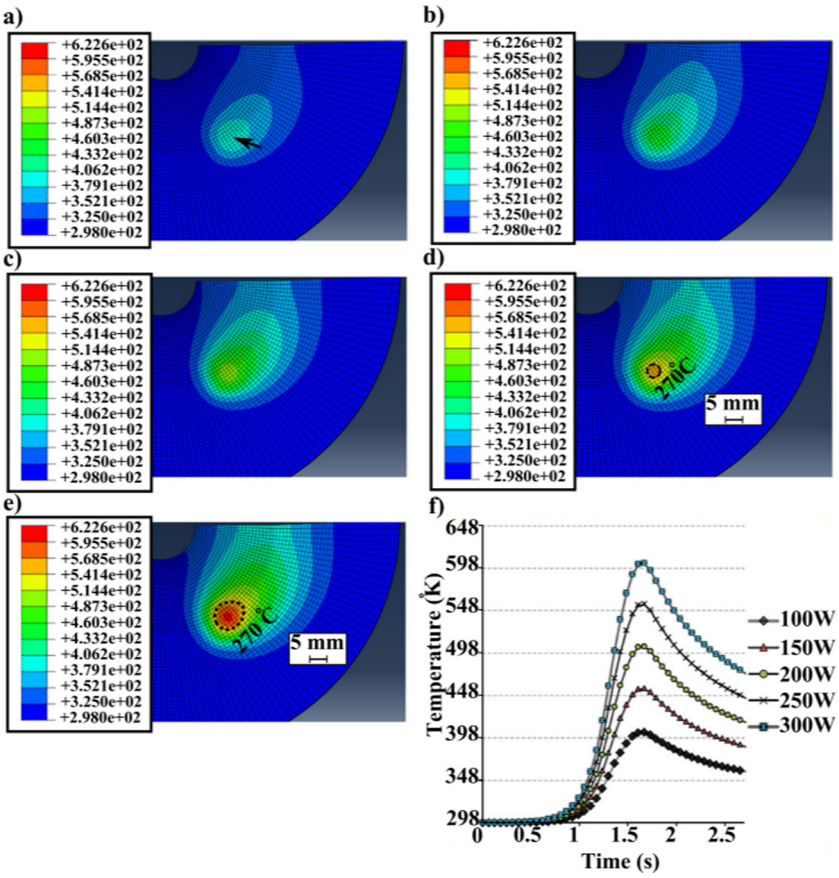

Fig. 11 FE results of temperature distributions under laser heating considering different laser power (**a**–**e**) and temperature evolution for a particular node (**f**) [9]

direction and rotate around the z direction at the center point of the tool. The three different tool positions of friction heat generation (SDV44) are depicted in Fig. 13. Figure 14 describes the temperature evolution at the elements corresponding to the three tool positions for forming 70° wall angle. The FE results showed that the maximum temperatures occurred at the corners (147 °C) and in the wall areas (122 °C) which were in good agreement with the experimental measurements. The formability decreased as the tool step-down or tool radius increased.

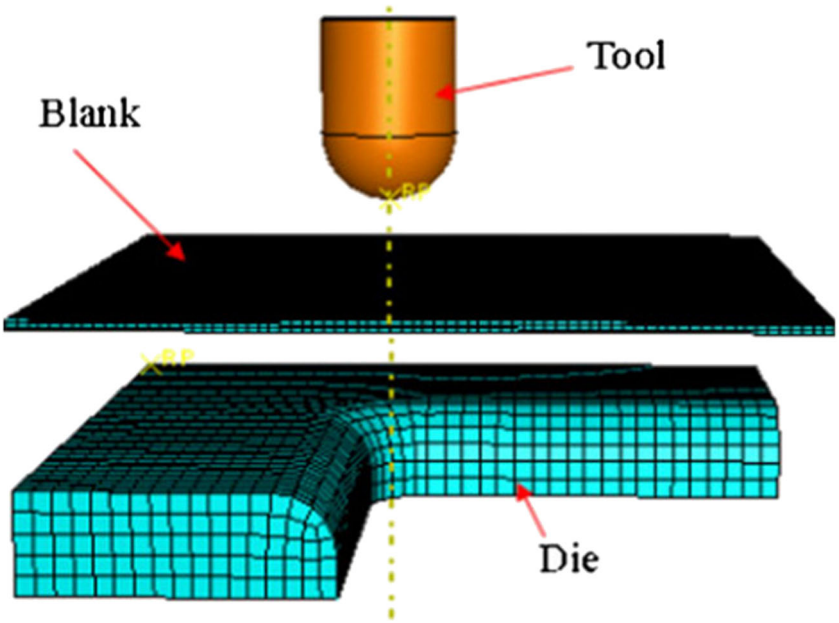

Fig. 12 Finite element model for friction heat-assisted ISF [19]

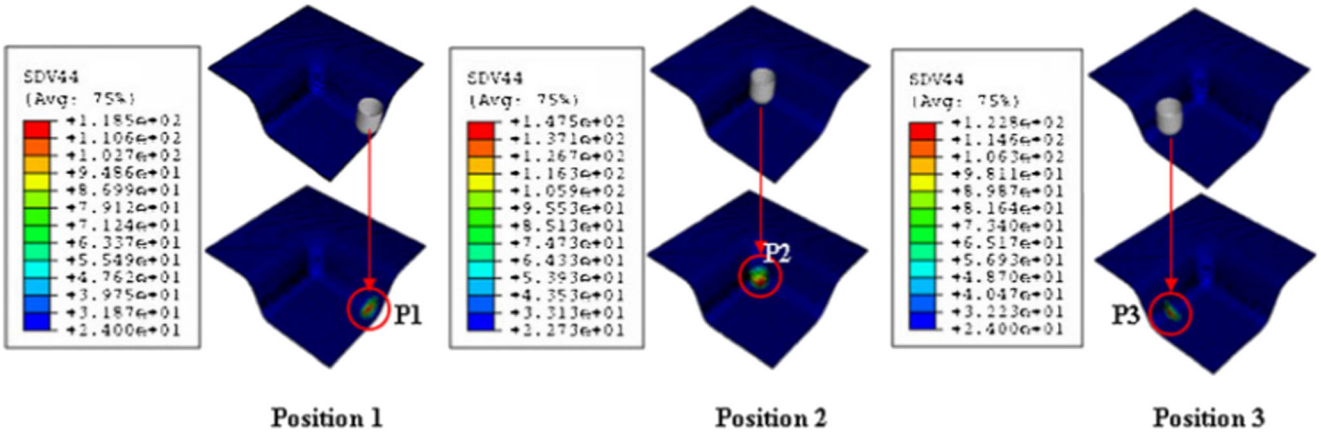

Fig. 13 The three different tool positions of friction heat generation [19]

Fan et al. [39] established a finite element model for electric heat-assisted ISF using MSC.Marc software, in which electricity-thermal-mechanical coupling model and hexahedral element SOLID7 were used. The equivalent thermal strain contours of the final step are depicted in Fig. 15, which shows that a thermal strain conduction and diffusion track was left behind after the tool traveling, and then the thermal strain gradually spread to the surrounding area and decreased. The evolution of the thermal strain for a selected node is given in Fig. 16. It is noted that the thermal strain of the sheet metal increases dramatically by electric heating. After the tool passing, the thermal strain decreases slowly. Given the thermal strain, the reverse bending of the sheet will occur. FE results further revealed that stresses are quite complex including tensile, compress, and shear stress, mainly dominated by compressive stress. Therefore, electric heat-assisted ISF has a large internal stress leading to complex thermoplastic deformation.

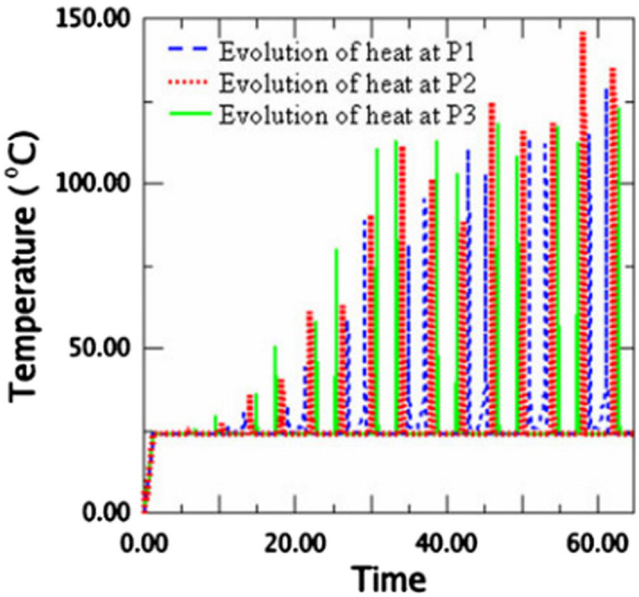

Fig. 14 Temperature evolution at the elements corresponding to the three tool positions [19]

Honarpisheh et al. [44] performed a numerical investigation of electric hot ISF of Ti-6Al-4V. In the FE model, the behavior of the stress-strain of Ti-6Al-4V was described by Johnson-Cook constitutive model. In addition, the sheet metal was modeled by eight-node trilinear displacement and temperature (thermally coupled brick) elements with reduced integration and hourglass control (C3D8RT). The stress and temperature distributions of FE simulation are depicted in Figs. 17 and 18. It was concluded that the current amperage, feed rate, and step-down size are the main and most important variables in the electrical hot ISF, which could be controlled to form a perfect part with wall angle larger than 45°. Another similar work performed by Pacheco and Silveira [54] was also focused on the FE modeling of electrical hot ISF with software RADIOSS, in which the stress-strain behavior of AA1050 alloy was also described by Johnson-Cook constitutive model. They stated that electrical hot ISF with preheating can increase the overall formability compared with the same process without preheating.

Considering the limitations of local electric heating ISF, Li et al. [50] proposed a new design for global electric heating ISF. In the study, the thermal-electrical coupling FE simulation of deforming TC4 Ti alloy was performed to analyze the influences of different currents on forming temperatures. Eight-node linear coupled thermal-electrical elements were used to model the sheet metal, steel plates, ceramic plates, and the ceramic base. The details of FE model are illustrated in Fig. 19. The temperatures predicted by FE model are validated by actual experimental data with different current values, which shows good agreements with each other.

3.3 Empirical models

The analytical models are sometimes cumbersome and unsatisfactory, while numerical simulations are time-

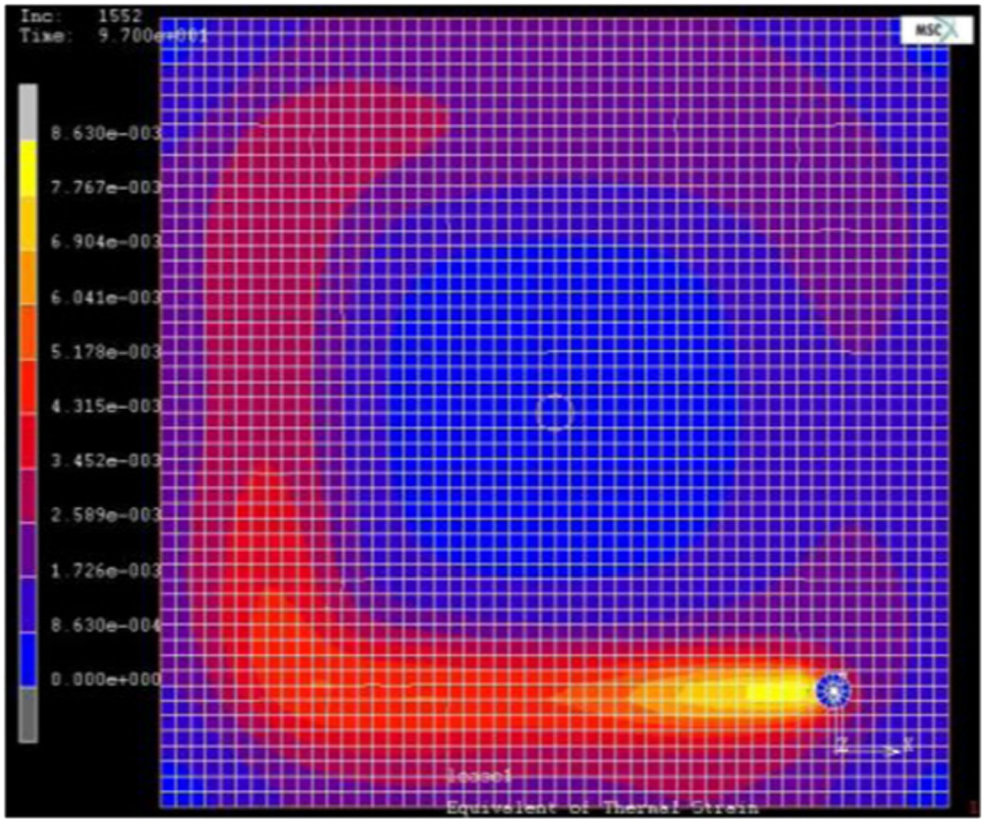

Fig. 15 Thermal strain of the final step [39]

consuming. Based on the design of experiment (DoE), Ambrogio et al. [26] established an empirical model using response surface methodology (RSM) to predict the temperature, as well as to determine the correlations between temperature and process parameters for friction heat-assisted ISF. The similar approach was also used by Khazaali and Fereshteh-Saniee [45] and Li et al. [49] to empirically model the electric heat-assisted ISF.

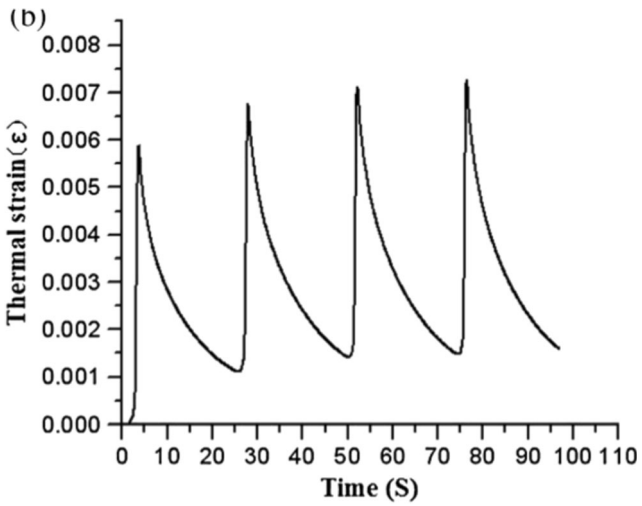

Fig. 16 The evolution of thermal strain in a selected node [39]

3.4 Summary

Current analytical analysis has largely focused on electric heat-assisted ISF process. These simplified thermal models have been established to predict the forming temperature based on fundamental energy balance relation without considering complex nonlinear thermomechanical coupling behavior involved in HA-ISF. Therefore, there is a need to develop more efficient numerical models to predict the material temperatures, dimensions, and properties that are changing both in time and space depending on many process parameters. Some FE models were well established for HA-ISF, such as laser-assisted, friction-heat-assisted, and electric heat-assisted processes. Setting up of these FE models requires rich data from experimental tests that need to be done for particular batch of materials, which can be expensive for some application alloys such as medical grade titanium. Thus, material database for HA-ISF can be established. As the thermomechanical model is integrated into the FE model, the computational times have usually increased, which in turn lowers the efficiency of FE analysis. Hence, there is room for significant improvement. In addition, the thermomechanical failure prediction for HA-ISF using numerical models has only been achieved to a limited extent and improved constitutive laws are needed to further develop. Future work in numerical modeling needs to focus on improving current

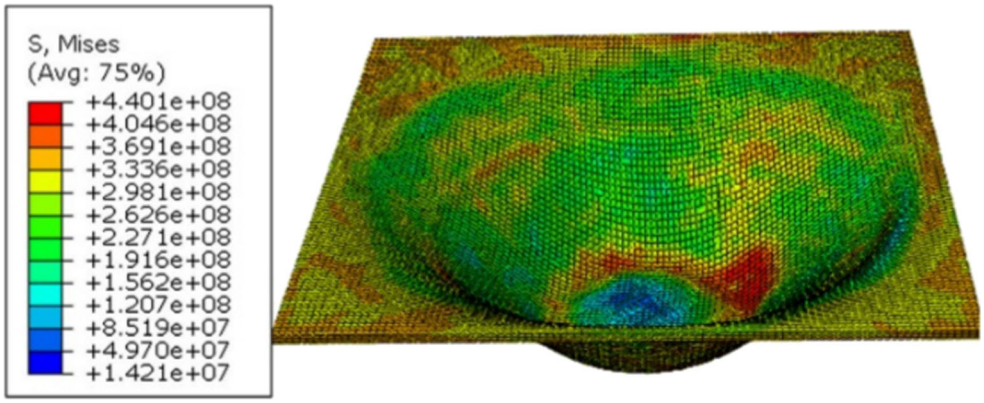

Fig. 17 Stress distribution [44]

limitations in simulation time, prediction of accuracy, constitutive laws, and failure prediction. Additionally, empirical models built based on experimental data could be applied to provide a fast estimation of outputs in HA-ISF, thereby facilitating the future design of HA-ISF.

4 Potential applications of HA-ISF

Over the past decade, some examples of applications of ISF have been witnessed. However, the direct industrial use of ISF is still limited, in which the use of HA-ISF as a hybrid forming technology based on basic ISF has not been documented yet in current literature. The academia is making great efforts to expand the application areas of ISF. The achievements in typical fields such as biomedical, automotive, and transportation are briefly summarized in this section. Then, the potential use of HA-ISF to these fields is envisaged.

4.1 Biomedical applications

The demands of fast fabrication of customized biomedical implants have stimulated the use of ISF in this field. Specific applicable cases have manifested its practicability, including ankle orthosis (Ambrogio et al. [62]); cranial plate (Duflou et al. [63], Bagudanch et al. [64], Lu et al. [65], Behera et al. [66]); facial implant (Duflou et al. [67], Araujo et al. [68]); palate, knee, and backseat prosthesis (Oleksik et al. [69], Fiorentino et al. [70, 71], Eksteen et al. [72, 73]); and clavicle implant (Vanhove et al. [74]). The materials used in these biomedical applications include Ti alloys (Duflou et al. [67], Oleksik et al. [69], Fiorentino et al. [71], Eksteen et al. [72, 73], Behera et al. [66]) and bio-polymers (Bagudanch et al. [64], Fiorentino et al. [70]). Formability is one of the big challenges to deform such kind of materials to freeform 3D shapes, followed by other constrains such as geometric accuracy and surface quality.

4.2 Automotive and transportation applications

Apart from biomedical applications, manufacture of different kinds of prototyping components in the areas of automotive, transportation, and aerospace has also been documented. In the automotive field, a car fender part was made by Bambach et al. [75]. A tail-light bracket for a car was made by Li et al. [76] using multi-pass-forming strategies of ISF. In the transportation field, a 1/8 scaled model of a Japanese Shinkansen bullet train was manufactured by AMINO Corporation [3].

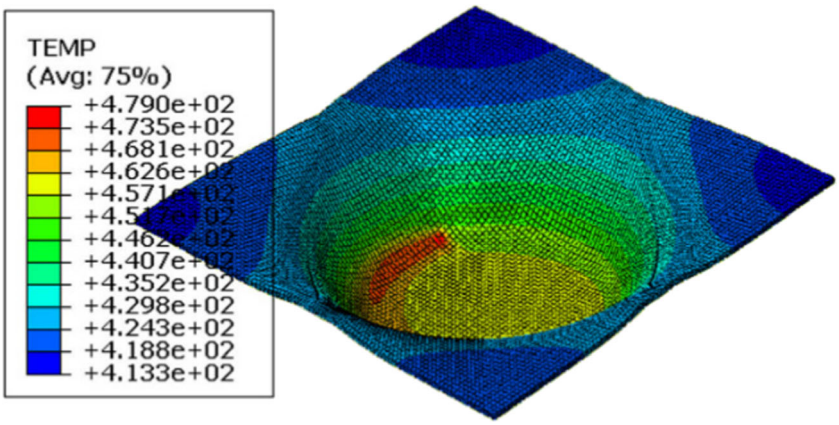

Fig. 18 Temperature distribution [44]

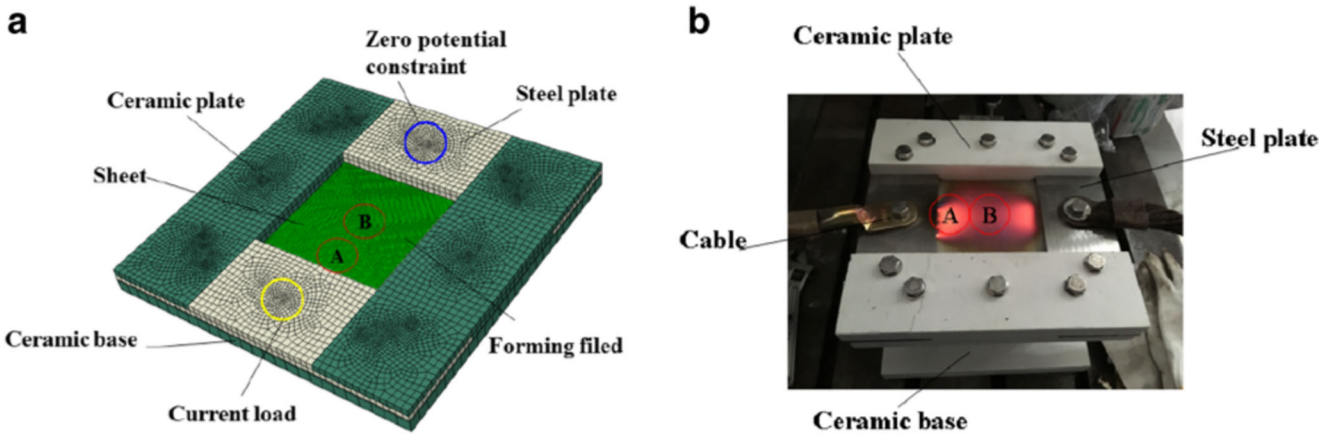

Fig. 19 Illustration for heating process simulation. **a** FE model. **b** Experimental setup [50]

4.3 Summary

The wide scale industrial use for C-ISF is still rare, while the industrial application of HA-ISF has not been reported so far. However, as a promising hybrid rapid prototyping sheet-forming technology, HA-ISF has drawn attention from academia. Of particular interest, in biomedical and aerospace areas, lots of hard-to-work alloys and polymers are widely applied, which will boost the potential use of HA-ISF to enhance the formability and forming accuracy of such materials, thereby overcoming the process limits of C-ISF.

5 Conclusions and future research directions

The heat-assisted ISF methods, involving the fundamentals and modeling methodology, have been comprehensively reviewed in this paper. By introducing different physical heat-generated approaches to conventional ISF process, the formability and geometric accuracy of many hard-to-deform materials at room temperatures could be improved at elevated temperatures. In the developed HA-ISF methods, the reachable heated temperature is a very important indicator that determines what kind of materials could be deformed. The current studies have shown that laser heat, friction heat, electric heat, and induction heat could raise the temperature above 600 °C so that these methods can be applied to process very hard-to-work materials such as Ti alloys and high-strength steels. The heated temperature generated by other methods, like halogen lamp heat, hot air heat, oil heat, and combined heat, is usually below 400 °C. In this situation, materials such Mg and Al alloys could be effectively formed. Very recently, halogen lamp heat method has also been applied to the incremental forming of short carbon fiber-reinforced thermoplastics in Okada et al. [77], which opens a new way for HA-ISF with exploitation of composite materials. Among the HA-ISF methods, each one has its own advantages and disadvantages. It seems that electric heat-assisted ISF is more popular in published works with potentials such as more efficient in heating and temperature more easily being controlled than friction-heat method. However, the newly emerging induction heat-assisted ISF inherits the pros of electric heat-assisted ISF and at the same time overcomes the limitations, like severe surface wear of tool and sheet caused by electric sparks that occurred in electric heat-assisted ISF. Therefore, the use of induction heat-assisted ISF has shown significant promise and more future research in this direction will help enhance process limits of dealing with materials with high strength.

Effective and efficient prediction of HA-ISF is usually a difficult task to accomplish, but the predictable results do benefit the design of relevant HA-ISF process and further facilitate the control of the process with regard to process limits, sheet thickness, and geometric accuracy. The current state of the art in the modeling of HA-ISF involves analytical, numerical, and empirical methods. The established analytical models are mostly focused on the temperature prediction in the electric heat-assisted ISF based on the Joule's law and Ohm's law. They cannot facilitate the understanding of complex nonlinear thermomechanical coupling behavior involved in HA-ISF. To solve the limitations of analytical models, it is necessary to develop more efficient and effective numerical models that could accurately predict the outputs of HA-ISF and analyze the effects of process variables on the thermomechanical forming process. The FE models that were well established for laser heat-assisted, friction-heat assisted, and electric heat-assisted ISF processes are thoroughly reviewed in this research. It is noted that as the thermomechanical model is integrated into the FE model, the computational times have usually increased, which in turn lowers the efficiency of FE simulation. In the future research, improvement for boosting simulation speed is worth paying attention to. What is more, accurate thermomechanical failure prediction for HA-ISF with FE models has proven to be hard and only been achieved to a limited extent in current literature. Confronted with new

materials (such as high-strength steels and carbon fiber-reinforced composites) emerging in HA-ISF, it is necessary to further develop and modify the constitutive equations to enhance the process predictability. Additionally, new FE models should be carried out to contribute to the analysis of other HA-ISF, like induction heat-assisted ISF. Other than analytical and numerical methods, the empirical model is also investigated based on the extensive experimental data without considering the mechanism of HA-ISF that could provide a fast estimation of outputs in HA-ISF, thereby facilitating the preliminary design of HA-ISF.

Although some applications in the fields of biomedical, automotive, and transportation have been identified, the real commercial industrial use for C-ISF is still limited, let alone the industrial application of HA-ISF that has not been reported yet. However, the initial functional components in biomedical application have been successfully formed with C-ISF that has further boosted the potentials of HA-ISF to form more complex 3D medical parts with hard-to-work alloys and even new polymers that cannot be done with C-ISF. This will enhance the formability and geometric accuracy of such materials, thereby overcoming the process limits of C-ISF.

It is noted that HA-ISF, as a promising hybrid rapid prototyping sheet-forming technology, is still an on-going research topic, which needs to be extensively investigated in the future.

Funding information This research is supported by the Fundamental Research Funds for the Central Universities (WUT 2017IVA017 and 2017III047).

References

1. Li Y, Chen X, Liu Z, Sun J, Li F, Li J, Zhao G (2017) A review on the recent development of incremental sheet-forming process. Int J Adv Manuf Technol 92(5):2439–2462
2. Duflou JR, Habraken A-M, Cao J, Malhotra R, Bambach M, Adams D, Vanhove H, Mohammadi A, Jeswiet J (2017) Single point incremental forming: state-of-the-art and prospects. Int J Mater Form
3. Behera AK, de Sousa RA, Ingarao G, Oleksik V (2017) Single point incremental forming: an assessment of the progress and technology trends from 2005 to 2015. J Manuf Process 27:37–62
4. McAnulty T, Jeswiet J, Doolan M (2017) Formability in single point incremental forming: a comparative analysis of the state of the art. CIRP J Manuf Sci Technol 16:43–54
5. Duflou JR, Callebaut B, Verbert J, De Baerdemaeker H (2007) Laser assisted incremental forming: formability and accuracy improvement. CIRP Ann 56(1):273–276
6. Duflou JR, Callebaut B, Verbert J, De Baerdemaeker H (2008) Improved SPIF performance through dynamic local heating. Int J Mach Tools Manuf 48(5):543–549
7. Callebaut, B., (2009) Sheet metal forming by laser forming and laser assisted incremental forming. Ph.D. thesis Katholieke Universiteit Leuven, Belgium
8. Göttmann A, Diettrich J, Bergweiler G, Bambach M, Hirt G, Loosen P, Poprawe R (2011) Laser-assisted asymmetric incremental sheet forming of titanium sheet metal parts. Prod Eng 5(3):263–271
9. Göttmann A, Bailly D, Bergweiler G, Bambach M, Stollenwerk J, Hirt G, Loosen P (2013) A novel approach for temperature control in ISF supported by laser and resistance heating. Int J Adv Manuf Technol 67(9):2195–2205
10. Mohammadi A, Vanhove H, Van Bael A, Duflou JR (2016) Towards accuracy improvement in single point incremental forming of shallow parts formed under laser assisted conditions. Int J Mater Form 9(3):339–351
11. Mohammadi A, Qin L, Vanhove H, Seefeldt M, Van Bael A, Duflou JR (2016) Single point incremental forming of an aged AL-cu-mg alloy: influence of pre-heat treatment and warm forming. J Mater Eng Perform 25(6):2478–2488
12. Mohammadi A, Vanhove H, Van Bael A, Seefeldt M, Duflou JR (2016) Effect of laser transformation hardening on the accuracy of SPIF formed parts. ASME J Manuf Sci Eng 139(1):011007–011007-12
13. Kim SW, Lee YS, Kang SH, Lee JH (2007) Incremental forming of Mg alloy sheet at elevated temperatures. J Mech Sci Technol 21(10):1518–1522
14. Ji YH, Park JJ (2008) Incremental forming of free surface with magnesium alloy AZ31 sheet at warm temperatures. Trans Nonferrous Metals Soc China 18:s165–s169
15. Ji YH, Park JJ (2008) Formability of magnesium AZ31 sheet in the incremental forming at warm temperature. J Mater Process Technol 201(1):354–358
16. Galdos L, Argandona ESD, Ulacia I, Arruebarrena G (2012) Warm incremental forming of magnesium alloys using hot fluid as heating media. Key Eng Mater 504-506:815–820
17. Durante M, Formisano A, Langella A, Capece Minutolo FM (2009) The influence of tool rotation on an incremental forming process. J Mater Process Technol 209(9):4621–4626
18. Park J, Kim J, Park N, Kim Y (2009) Study of forming limit for rotational incremental sheet forming of magnesium alloy sheet. Metall Mater Trans A 41(1):97
19. Nguyen D-T, Park J-G, Kim Y-S (2010) Combined kinematic/isotropic hardening behavior study for magnesium alloy sheets to predict ductile fracture of rotational incremental forming. Int J Mater Form 3(1):939–942
20. Nguyen D-T, Park J-G, Kim Y-S (2010) Ductile fracture prediction in rotational incremental forming for magnesium alloy sheets using combined kinematic/isotropic hardening model. Metall Mater Trans A 41(8):1983–1994
21. Otsu M, Matsuo H, Matsuda M, Takashima K (2010) Friction stir incremental forming of aluminum alloy sheets. Steel Res Int 81(9):942–945
22. Otsu M, Ichikawa T, Matsuda M, Takashima K (2011) Development of friction stir incremental forming. J Jpn Soc Technol Plast 52(603):490–494
23. Xu D, Wu W, Malhotra R, Chen J, Lu B, Cao J (2013) Mechanism investigation for the influence of tool rotation and laser surface texturing (LST) on formability in single point incremental forming. Int J Mach Tools Manuf 73:37–46
24. Xu D, Lu B, Cao T, Chen J, Long H, Cao J (2014) A comparative study on process potentials for frictional stir- and electric hot-assisted incremental sheet forming. Proc Eng 81:2324–2329
25. Ambrogio G, Gagliardi F, Bruschi S, Filice L (2013) On the high-speed single point incremental forming of titanium alloys. CIRP Ann 62(1):243–246

26. Ambrogio G, Gagliardi F (2015) Temperature variation during high speed incremental forming on different lightweight alloys. Int J Adv Manuf Technol 76(9):1819–1825
27. Ambrogio G, Ciancio C, Filice L, Gagliardi F (2016) Theoretical model for temperature prediction in incremental sheet forming—experimental validation. Int J Mech Sci 108-109:39–48
28. Buffa G, Campanella D, Fratini L (2013) On the improvement of material formability in SPIF operation through tool stirring action. Int J Adv Manuf Technol 66(9):1343–1351
29. Davarpanah MA, Mirkouei A, Yu X, Malhotra R, Pilla S (2015) Effects of incremental depth and tool rotation on failure modes and microstructural properties in single point incremental forming of polymers. J Mater Process Technol 222:287–300
30. Wang J, Li L, Jiang H (2016) Effects of forming parameters on temperature in frictional stir incremental sheet forming. J Mech Sci Technol 30(5):2163–2169
31. Baharudin, B. T. H. T.; Azpen, Q. M.; Sulaima, Shamsuddin; Mustapha, F., Experimental investigation of forming forces in frictional stir incremental forming of aluminum alloy AA6061-T6. Metals 2017**,** 7 (11), 1–15
32. Liu Z (2017) Friction stir incremental forming of AA7075-O sheets: investigation on process feasibility. Proc Eng 207:783–788
33. Uheida EH, Oosthuizen GA, Dimitrov DM, Bezuidenhout MB, Hugo PA (2018) Effects of the relative tool rotation direction on formability during the incremental forming of titanium sheets. Int J Adv Manuf Technol 96:3311–3319
34. Ambrogio G, Filice L, Manco GL (2008) Warm incremental forming of magnesium alloy AZ31. CIRP Ann 57(1):257–260
35. Ambrogio G, Filice L, Gagliardi F (2012) Formability of lightweight alloys by hot incremental sheet forming. Mater Des 34: 501–508
36. Fan G, Gao L, Hussain G, Wu Z (2008) Electric hot incremental forming: a novel technique. Int J Mach Tools Manuf 48(15):1688–1692
37. Fan G, Sun F, Meng X, Gao L, Tong G (2010) Electric hot incremental forming of Ti-6Al-4V titanium sheet. Int J Adv Manuf Technol 49(9):941–947
38. Fan G, Gao L (2014) Mechanical property of Ti-6Al-4V sheet in one-sided electric hot incremental forming. Int J Adv Manuf Technol 72(5):989–994
39. Fan G, Gao L (2014) Numerical simulation and experimental investigation to improve the dimensional accuracy in electric hot incremental forming of Ti–6Al–4V titanium sheet. Int J Adv Manuf Technol 72(5):1133–1141
40. Le Van S, Nguyen Thanh N (2013) Hot incremental forming of magnesium and aluminum alloy sheets by using direct heating system. Proc Inst Mech Eng B J Eng Manuf 227(8):1099–1110
41. Shi X, Gao L, Khalatbari H, Xu Y, Wang H, Jin L (2013) Electric hot incremental forming of low carbon steel sheet: accuracy improvement. Int J Adv Manuf Technol 68(1):241–247
42. Adams D, Jeswiet J (2014) Single point incremental forming of 6061-T6 using electrically assisted forming methods. Proc Inst Mech Eng B J Eng Manuf 228(7):757–764
43. Bao W, Chu X, Lin S, Gao J (2015) Experimental investigation on formability and microstructure of AZ31B alloy in electropulse-assisted incremental forming. Mater Des 87:632–639
44. Honarpisheh M, Abdolhoseini MJ, Amini S (2016) Experimental and numerical investigation of the hot incremental forming of Ti-6Al-4V sheet using electrical current. Int J Adv Manuf Technol 83(9):2027–2037
45. Khazaali H, Fereshteh-Saniee F (2016) A comprehensive experimental investigation on the influences of the process variables on warm incremental forming of Ti-6Al-4V titanium alloy using a simple technique. Int J Adv Manuf Technol 87(9):2911–2923
46. Liu R, Lu B, Xu D, Chen J, Chen F, Ou H, Long H (2016) Development of novel tools for electricity-assisted incremental sheet forming of titanium alloy. Int J Adv Manuf Technol 85(5): 1137–1144
47. Najafabady SA, Ghaei A (2016) An experimental study on dimensional accuracy, surface quality, and hardness of Ti-6Al-4 V titanium alloy sheet in hot incremental forming. Int J Adv Manuf Technol 87(9):3579–3588
48. Xu DK, Lu B, Cao TT, Zhang H, Chen J, Long H, Cao J (2016) Enhancement of process capabilities in electrically-assisted double sided incremental forming. Mater Des 92:268–280
49. Li Z, Lu S, Zhang T, Zhang C, Mao Z (2017) 1060 Al electric hot incremental sheet forming process: analysis of dimensional accuracy and temperature. Trans Indian Inst Metals
50. Li Z, Lu S, Zhang T, Zhang C, Mao Z (2018) Electric assistance hot incremental sheet forming: an integral heating design. Int J Adv Manuf Technol
51. Magnus CS (2017) Joule heating of the forming zone in incremental sheet metal forming: part 1. Int J Adv Manuf Technol 91(1):1309–1319
52. Magnus CS (2017) Joule heating of the forming zone in incremental sheet metal forming: part 2. Int J Adv Manuf Technol 89(1):295–309
53. Min J, Seim P, Störkle D, Thyssen L, Kuhlenkötter B (2017) Thermal modeling in electricity assisted incremental sheet forming. Int J Mater Form 10(5):729–739
54. Pacheco PAP, Silveira ME (2017) Numerical simulation of electric hot incremental sheet forming of 1050 aluminum with and without preheating. Int J Adv Manuf Technol
55. Meier H, Magnus C, Buff B, Zhu J (2013) Tool concepts and materials for incremental sheet metal forming with direct resistance heating. Key Eng Mater 549:61–67
56. Al-Obaidi A, Kräusel V, Landgrebe D (2016) Hot single-point incremental forming assisted by induction heating. Int J Adv Manuf Technol 82(5):1163–1171
57. Al-Obaidi A, Kräusel V, Landgrebe D (2017) Induction heating validation of dieless single-point incremental forming of AHSS. J Manuf Mater Process 1(1):1–10
58. Ambrogio G, Gagliardi F, Chamanfar A, Misiolek WZ, Filice L (2017) Induction heating and cryogenic cooling in single point incremental forming of Ti-6Al-4V: process setup and evolution of microstructure and mechanical properties. Int J Adv Manuf Technol 91(1):803–812
59. Palumbo G, Brandizzi M (2012) Experimental investigations on the single point incremental forming of a titanium alloy component combining static heating with high tool rotation speed. Mater Des 40:43–51
60. Zhang Q, Guo H, Xiao F, Gao L, Bondarev AB, Han W (2009) Influence of anisotropy of the magnesium alloy AZ31 sheets on warm negative incremental forming. J Mater Process Technol 209(15):5514–5520
61. Zhang Q, Xiao F, Guo H, Li C, Gao L, Guo X, Han W, Bondarev AB (2010) Warm negative incremental forming of magnesium alloy AZ31 sheet: new lubricating method. J Mater Process Technol 210(2):323–329
62. Ambrogio G, De Napoli L, Filice L, Gagliardi F, Muzzupappa M (2005) Application of incremental forming process for high customised medical product manufacturing. J Mater Process Technol 162-163:156–162
63. Duflou J.; Lauwers B.; Verbert J.; Gelaude F.; Tunckol Y.,(2005**)** Medical application of single point incremental forming: cranial plate manufacturing. *In: Proceedings of the 2nd international conference on advanced research in virtual and rapid prototyping*. 161–166
64. Bagudanch I, Lozano-Sánchez LM, Puigpinós L, Sabater M, Elizalde LE, Elías-Zúñiga A, Garcia-Romeu ML (2015) Manufacturing of polymeric biocompatible cranial geometry by single point incremental forming. Proc Eng 132:267–273

65. Lu B, Xu DK, Liu RZ, Ou H, Long H, Chen J (2015) Cranial reconstruction using double side incremental forming. Key Eng Mater 639:535–542
66. Behera AK, Lu B, Ou H (2016) Characterization of shape and dimensional accuracy of incrementally formed titanium sheet parts with intermediate curvatures between two feature types. Int J Adv Manuf Technol 83(5):1099–1111
67. Duflou JR, Behera AK, Vanhove H, Bertol LS (2013) Manufacture of accurate titanium Cranio-facial implants with high forming angle using single point incremental forming. Key Eng Mater 549:223–230
68. Araujo R, Teixeira P, Montanari L, Reis A, Silva MB, Martins PA (2014) Single point incremental forming of a facial implant. Prosthetics Orthot Int 38:369–378
69. Oleksik V.; Pascu A.; Deac C.; Fleaca R.; Roman M.; Bologa O., (2010) The influence of geometrical parameters on the incremental forming process for knee implants analyzed by numerical simulation. NUMIFORM **,** 1208–1215
70. Fiorentino A.; Marenda G.P.; Marzi R.; Ceretti E.; Kemmoku D.T.; Silva J.V.L., (2011) Rapid prototyping techniques for individualized medical prosthesis manufacturing. *In: Innovative developments in virtual and physical prototyping.* CRC Press , 589–594
71. Fiorentino A, Marzi R, Ceretti E (2012) Preliminary results on Ti incremental sheet forming (ISF) of biomedical devices: biocompatibility, surface finishing and treatment. Int J Mechatronics Manuf Syst 5:36–45
72. Eksteen P.D.; Van der Merwe A.F.,(2012**)** Incremental sheet forming (ISF) in the manufacturing of titanium based plate implants in the bio-medical sector. *In: Proceedings of the international conference on computers & industrial engineering (CIE 42)* 569–575
73. Eksteen P.D.,(2013) [Thesis (MScEng)] Development of incrementally formed patient-specific titanium knee prosthesis. *Stellenbosch University*
74. Vanhove H, Carette Y, Vancleef S, Duflou JR (2017) Production of thin shell clavicle implants through single point incremental forming. Proc Eng 183:174–179
75. Bambach M, Araghi BT, Hirt G (2009) Strategies to improve the geometric accuracy in asymmetric single point incremental forming. Prod Eng 3:145–156
76. Li JC, Shen JJ, Wang B (2013) A multipass incremental sheet forming strategy of a car taillight bracket. Int J Adv Manuf Technol 69:2229–2236
77. Okada M, Kato T, Otsu M, Tanaka H, Miura T (2018) Development of optical-heating-assisted incremental forming method for carbon fiber reinforced thermoplastic sheet-Forming characteristics in simple spot-forming and two-dimensional sheet-fed forming. J Mater Process Technol 256(6):145–153